NASA TECHNICAL MEMORANDUM

NASA TM X-62,434

NASA TM X- 62,434

THE ACCURACY OF FAR-FIELD NOISE OBTAINED BY THE MATHEMATICAL EXTRAPOLATION OF NEAR-FIELD NOISE DATA

Warren F. Ahtye and Steven Karel

Ames Research Center
Moffett Field, California 94035

and

U.S. Army Element NASA
Washington, D.C. 20546

July 1975

1. Report No.	2. Government Accession No.	3. Recipient's Catalog No.
TM X-62,434		

4. Title and Subtitle	5. Report Date
THE ACCURACY OF FAR-FIELD NOISE OBTAINED BY THE MATHEMATICAL EXTRAPOLATION OF NEAR-FIELD NOISE DATA	6. Performing Organization Code

7. Author(s)	8. Performing Organization Report No.
Warren F. Ahtye and Steven Karel	A-6077
	10. Work Unit No. 505-10-31

9. Performing Organization Name and Address	11. Contract or Grant No.
Ames Research Center, Moffett Field, Calif. 94035 — U.S. Army Element NASA, Washington, D.C. 20546	
	13. Type of Report and Period Covered: Technical Memorandum

12. Sponsoring Agency Name and Address	14. Sponsoring Agency Code
National Aeronautics and Space Administration, Washington, D.C. 20546	

15. Supplementary Notes

16. Abstract

This paper describes the results of an analytical study of the accuracy and limitations of a technique that permits the mathematical extrapolation of near-field noise data to far-field conditions. The effects of the following variables on predictive accuracy of the far-field pressure were examined: (1) number of near-field microphones; (2) length of source distribution; (3) complexity of near-field and far-field distributions; (4) source-to-microphone distance; and (5) uncertainties in microphone data and imprecision in the location of the near-field microphones. It is shown that the most important parameters describing predictive accuracy are the number of microphones, the ratio of source length to acoustic wavelength, L/λ, and the error in location of near-field microphones. If microphone measurement and location errors are not included, then far-field pressures can be accurately predicted up to L/λ values of 15 using approximately 50 microphones. For maximum microphone location errors of ±1 cm, only an accuracy of ±2-1/2 dB can be attained with approximately 40 microphones for the highest L/λ of 10. However, this restriction can be lifted to a large degree if more precise measurement techniques are used.

17. Key Words (Suggested by Author(s))	18. Distribution Statement
Aerodynamics transportation Aerodynamics	Unlimited STAR Category - 03, 02

19. Security Classif. (of this report)	20. Security Classif. (of this page)	21. No. of Pages	22. Price*
Unclassified	Unclassified	13	$3.25

*For sale by the National Technical Information Service, Springfield, Virginia 22151

THE ACCURACY OF FAR-FIELD NOISE OBTAINED BY THE MATHEMATICAL EXTRAPOLATION OF NEAR-FIELD NOISE DATA

Warren F. Ahtye
Ames Research Center, NASA, Moffett Field, California 94035

and

Steven Karel
U.S. Army Element NASA, Washington, D.C. 20546

Abstract. This paper describes the results of an analytical study of the accuracy and limitations of a technique that permits the mathematical extrapolation of near-field noise data to far-field conditions. The effects of the following variables on predictive accuracy of the far-field pressure were examined: (1) number of near-field microphones; (2) length of source distribution; (3) complexity of near-field and far-field distributions; (4) source-to-microphone distance; and (5) uncertainties in microphone data and imprecision in the location of the near-field microphones. It is shown that the most important parameters describing predictive accuracy are the number of microphones, the ratio of source length to acoustic wavelength, L/λ, and the error in location of near-field microphones. If microphone measurement and location errors are not included, then far-field pressures can be accurately predicted up to L/λ values of 15 using approximately 50 microphones. For maximum microphone location errors of ±1 cm, only an accuracy of ±2-1/2 dB can be attained with approximately 40 microphones for the highest L/λ of 10. However, this restriction can be lifted to a large degree if more precise measurement techniques are used.

INTRODUCTION

The measurement of the effects of forward speed on the noise generated by a full-scale propulsion system can be done by two complementary techniques. The first is testing of the propulsion system in large-scale wind tunnels such as the NASA Ames 40- by 80-Ft Wind Tunnel (1,2). The second technique is flight testing of aircraft containing or carrying the propulsion system (3). The major portion of these forward speed measurements should be made in wind tunnels because of lower costs, shorter times for configuration changes, and most important, a precise control of aircraft and engine parameters that results in more accurate and consistent noise data.

However, there are certain limitations in using wind tunnels with closed test sections. These limitations can be attributed to the following factors: (1) limited size of the test section; (2) large reflectivity of the enclosing surfaces; (3) extraneous noise arriving at the microphone from the tunnel drive fans; and (4) extraneous noise generated at the microphone itself by turbulent fluctuations on the microphone body. The finite dimensions of the test section physically limit the maximum source-to-microphone distance for a given direction. Under certain circumstances, the last two factors can restrict this distance even more. The large reflectivity of steel walls in large-scale wind tunnels results in the formation of a reverberant field that is relatively uniform within the test section (4). The noise within the test section that comes from the wind tunnel drive fan and the noise generated at the microphone are also independent of test section location. This is in contrast to the direct field from the propulsion system, which falls off rapidly as source-to-microphone distance increases. Under certain circumstances, diagnostic techniques can be used to minimize the effects of reverberant noise or other extraneous noises, so that the physical size of the test section would be the only restriction on the source-to-microphone distance. These diagnostic techniques are described by Soderman (5).

When the usefulness of these diagnostic techniques becomes marginal, then the only solution remaining is to minimize the reverberant and other extraneous noises by moving the microphones closer to the primary source (i.e., the propulsion system). Under these conditions the microphones are located in the near-field of the primary source.* However, far-field acoustic data are required for comparison with flight test data. As a consequence, an analytical technique is required to permit the extrapolation of near-field data to far-field conditions. This paper describes the accuracy and limitations of one such technique.

PREVIOUS INVESTIGATIONS

Theoretical Investigations

The problem of predicting far-field pressures from near-field measurements has received considerable attention from theoretical acousticians. Initially, the Helmholtz integral and Green's function approaches were used for situations where there was a specification of the continuous distribution of near-field pressures on a surface surrounding the source. However, these approaches are not suitable for wind tunnel applications where measurements are taken at discrete points. Suitable approaches do exist that utilize the numerical solutions of partial differential equations at discrete boundary points. One of the simplest of these is the boundary-collocation method, applied to the prediction of far-field pressures from near-field data, by Meggs (6) and Butler (7).

*The distinction between near-field and far-field is discussed in the appendix.

The most comprehensive application of this method is described by Butler (8,9). Butler applied the method to coherent sources (each monopole emitting in phase with the other monopoles) and partially coherent sources (each monopole emitting with differing phase, but with defined space correlations between phases from the other monopoles). Butler used two slightly different approaches. The first (8) requires the simultaneous measurement of near-field pressure amplitudes and phases, whereas the second (9) requires the use of magnitude only, but with an attendant increase in the number of microphones. Butler's calculations are more applicable to underwater acoustics than aircraft propulsion noise because of the range of wavelengths used. For example, his source lengths are of the order of 2λ, where λ is the acoustic wavelength. In contrast, aircraft propulsion systems have ratios of L/λ ranging from 0.2 to 100.

The approach Butler took was to assume a distribution of three monopoles in line as his source. From this known distribution, both the exact near-field and far-field pressures are calculated, with the exact near-field pressures taking on the role of error-free microphone data. Boundary collocation is then applied to the near-field data to yield the approximated far-field pressures. The latter is compared with the previously calculated exact far-field pressures to determine the accuracy of the method. On the basis of his results (8), for the simple monopole configuration and limited wavelengths, Butler (8) came to the following conclusion: "A reasonable criterion for a good prediction [of the far-field pressures] would be that N [number of near-field microphones] must be at least kL, where L is the length of the line or roughly $N > 6L/\lambda$". In addition, Butler showed that for a given source configuration and a given number of microphones, the accuracy of the prediction for the partially coherent source is only slightly better than that for the coherent source.

Experimental Investigation

An experimental verification of Butler's boundary-collocation method was attempted by Bies and Scharton (10). They used a complex noise source consisting of a loudspeaker covered with a perforated faceplate. The overall dimension of the source was 1.5λ. A total of 15 microphones was used to measure the magnitudes of the near-field pressures at a distance of approximately λ and the magnitudes of the far-field pressures at 11λ. The sound source was excited with pure tone at 5 kHz and with 1/10 octave pink noise centered at 5 kHz. They used Butler's second approach (9) utilizing amplitudes of the near-field microphones for the collocation calculation, rather than the more accurate amplitude and phase approach (8).

In each case the calculation resulted in nonsensical values of the collocation coefficients which characterize the source. Bies and Scharton attributed this failure to either an insufficient number of microphones or inherent inaccuracies in the microphones measurements of the near-field amplitudes. No attempt was made to investigate the effects of these two variables. In any event, they came to the conclusion that "Analytical techniques for calculating the far field directivity on the basis of near-field acoustic data do not appear promising". In a subsequent section we will attempt to show why Bies and Scharton did not succeed.

APPROACH TO PROBLEM

General Approach and Scope

The approach we used in this work is similar to the one used by Butler (8). In the first phase, we assume a linear distribution of multipoles. From this known distribution, both the exact near-field and far-field pressure amplitudes and phases are calculated. The exact near-field pressure amplitudes and phases at points corresponding to microphone locations are used as input data in the boundary-collocation computation of the far-field pressures. These approximated far-field pressures are then compared with the previously calculated exact far-field pressures to determine the accuracy of the method. However, the scope of this study is much wider than that of reference 8; for example, it covers the range of acoustic wavelengths that is of primary interest in the examination of full-scale aircraft propulsion noise (λ from 1 m to 0.05 m). In addition, we investigate the changes in the accuracy of the method due to changes in the following parameters: (1) the number of near-field microphones; (2) the length of the source distribution; (3) source-to-microphone distance; and (4) the types of multipoles (e.g., dipoles, quadrupoles). In one respect, the scope is more limited than that of reference 8. For all cases described in this paper the multipoles were assumed to be emitting coherently. Butler's comparison of coherent and partially coherent sources indicates that this restriction would give us a measure of predictive accuracy that would be slightly lower than that based on partially coherent sources for his configurations. In the second phase, we investigate the changes in the accuracy of the extrapolation due to the presence of random errors in near-field microphone data and in the locations of these microphones.

Mathematical Background

The success of the boundary-collocation method hinges on an accurate solution of the collocation coefficients that are characteristic of the noise source. These complex coefficients are used in the direct computation of the approximate far-field pressure amplitude and phase. Before we can meaningfully discuss the results of the collocation method, we must have a general idea of the mathematical bases of these coefficients. The governing field equation for harmonic waves emanating from a distribution of sources is the Helmholtz equation

$$\nabla^2 p + k^2 p = 0 \qquad (1)$$

where p is the complex pressure at any field point, and k is the wave number, equal to $2\pi/\lambda$. An exact solution of this equation can be obtained by the standard technique of separation of

variables for certain coordinate systems. For the special case of an axisymmetric distribution, the expansion series for the complex pressure at any given field point is

$$p(r,\theta) = \sum_{n=0}^{\infty} a_n P_n(\cos\theta) h_n^{(1)}(kr) \qquad (2)$$

in terms of spherical coordinates. Here $P_n(\cos\theta)$ is the Legendre polynomial of order n, and $h_n^{(1)}$ is the spherical Hankel function. The pressure at any field point can be approximated by the finite sum

$$p(r,\theta) \cong \sum_{n=0}^{N-1} a_n P_n(\cos\theta) h_n^{(1)}(kr) \qquad (3)$$

if the remainder term

$$D_N(r,\theta) = \left| \sum_{n=N}^{\infty} a_n P_n(\cos\theta) h_n^{(1)}(kr) \right| \qquad (4)$$

is small for the entire space.

At this point the boundary-collocation approximation is made. Let us assume that the acoustic pressure amplitude and phase are known at N specified points (i.e., specified θ_i and r_i, $i = 1, 2, \ldots, N$), giving us values for $p(r_i,\theta_i)$, $P_n(\cos\theta_i)$, and $h_n^{(1)}(kr_i)$. Then the approximation is made that

$$p(r_i,\theta_i) = \sum_{n=0}^{N-1} a_n' P_n(\cos\theta_i) h_n^{(1)}(kr_i), \quad i = 1,2,\ldots,N \qquad (5)$$

where a_n' is the complex collocation coefficient. These coefficients can be found by solving the finite set of simultaneous linear equations (eq. (3)). Whereas a_n in equation (2) is an exact characterization of the noise source, a_n' in equation (5) is only an approximation. Once the N values of a_n' are found from the near-field data, these collocation coefficients, along with the far-field coordinates, are used in equation (5) to find the far-field pressure.

An analysis of the rate at which the series (eq. (2)) converges (which tells us how fast D_n goes to zero) would be the proper approach to determine the accuracy of the collocation method. However, this approach is rendered infeasible by the complicated nature of the functions involved. Therefore, it is necessary to employ the less precise, but more practical, techniques described in this paper.

Computational Limitations

At the beginning of this study we reproduced some of the results of reference 8 in order to check our computer program. The standard Gaussian elimination subroutine for the computation of the collocation coefficients was used. We encountered no difficulty with the relatively simple configurations of reference 8. When we progressed to more complicated configurations (e.g., 31 multipoles encircled by 30 microphones) the computer program yielded nonsensical values for the collocation coefficients. An analysis of our computer program by Galant (11) showed that the problem could be attributed to the fact that the set of linear equations containing the collocation coefficients was near-singular. Galant suggested that we replace the Gaussian elimination subroutine with a relatively new subroutine using the concept of singular value decomposition (12,13). We subsequently did use this new subroutine and the resulting values of the far-field pressures became reasonable. On the basis of our experience, we strongly recommend the use of singular value decomposition for any application of the collocation method to configurations that are not extremely simple.

Our computer program contains another potential numerical limitation. The subroutines for computing spherical Bessel functions by recurrence relations become inaccurate when $j_n(kr)$ approaches 10^{-8}. This limitation interfered with our calculations for only a few unimportant cases. However, this factor should be noted by those wishing to conduct further investigations.

RESULTS

Basic Configuration

The basic source-microphone configuration used for the greater part of the analysis is shown in figure 1. The 3-m length of the source was chosen to correspond to the length of the major noise producing region of a typical jet exhaust. This hypothetical source is made up of 6 monopoles, as well as 13 dipoles and 12 lateral quadrupoles with their axes aligned parallel to the line joining the multipoles. The strengths of these multipoles were chosen at random with the source strengths varying by a factor of 10. The near-field microphones are arranged in a semicircular arc of 2-m radius with θ ranging from 5° to 175°, unless otherwise specified. The far-field pressures are always taken at points along a semicircular arc of 50-m radius, with θ ranging from 5° to 175° in increments of 5°.

Before we determine the accuracy of the collocation method, we should compare the shapes of the exact far-field and near-field pressures for the base configuration in order to give us some indication of the predictive task that will be imposed on this method. Both sets of exact data are compared in figure 2, for a range of wavelengths. Both sets have been normalized so that they have the same peak value. For the longest λ (1 m) the shapes are similar for angles greater than 20°, with both distributions exhibiting four distinct peaks of varying size. In contrast, the distributions at lower λ are not similar. For example, at a λ of 0.2 m the exact near-field has one predominant peak at approximately 3°, whereas the exact far-field has five major peaks of approximately the same magnitude. It is obvious from these plots that the shorter λ will present a greater predictive challenge.

Measure of Predictive Accuracy

We must have some criterion for determining the predictive accuracy of the collocation method. In this study we used a simple mean predictive

error that is determined as follows. The local predictive error is defined as

$$\delta SPL_l(\theta_{far}) = 20 \cdot \log_{10}(p_{collocation}/p_{exact}) \quad (6)$$

where $p_{collocation}$ and p_{exact} are local values. The quantity δSPL_l can have both positive and negative values. The mean predictive error, δSPL, is simply the mean of the absolute values of the local errors at the 35 far-field points.

The mean predictive error can give misleading indications, as it gives equal weight to errors in peak regions of the distribution and to errors in valleys, where the pressures may be orders of magnitude smaller than the peak pressures. This occurs more frequently for large values of the mean predictive error. Comparison between exact and predicted far-field pressures, for cases where $\delta SPL > 5$, shows relatively small discrepancies in peak regions, but extremely large ones in valleys. An example of this situation will be shown in a subsequent section. A measure of accuracy which would circumvent this problem is a weighted mean using the following weighted local error:

$$\delta SPL_l(\theta_{far}) = \frac{p_{exact}}{p_{average}} \cdot 20 \cdot \log_{10}(p_{collocation}/p_{exact}) \quad (7)$$

where

$$p_{average} = \frac{1}{\pi} \int_0^{\pi} p_{exact}\, d\theta \quad (8)$$

Although we did not use such a weighted mean because of increased computational time, we recommend it for future investigations.

Number of Microphones

One of the obvious questions is, for a given source configuration, how does the predictive accuracy change as the number of microphones is increased? First, we should look at several comparisons of exact and approximated far-field pressures for the basic configuration (fig. 1). The cases are shown in figure 3. A good example of the predictive capability of the collocation method is shown in figure 3(a) where δSPL is essentially 0. The mean predictive error in figure 3(b) is 9.9 dB. There is very little agreement for any angle. In figure 3(c), δSPL is still relatively large at 5.5 dB. However, the comparative results would be acceptable except for θ below 20°. The predictive accuracy for the basic configuration is summarized in figure 4, where δSPL is plotted against the number of near-field microphones, N. For all wavelengths below 0.2 m, there is an error of approximately 10 dB if only 10 microphones are used. As N is increased, there is no discernible improvement, but just a slight fluctuation due to the changing near-field coordinates, as the microphone locations are changed. For all wavelengths, a point is eventually reached where δSPL begins to decrease. This transition point decreases with increasing λ. The decrease in δSPL is relatively slow for the shorter λ and extremely rapid for longer λ. At wavelengths below 0.10 m, there is a breakdown for large numbers of microphones (e.g., 86). This may be due to an inadequacy of the computer subroutine for solving a system of linear equations of large order.

From figure 4 we can determine the number of near-field microphones required to reach a certain level of accuracy by cross-plotting. Figure 5 shows the required N as a function of wavelength, with predictive errors of 1 dB and 3 dB. Superimposed on this figure is the curve $N = 6L/\lambda$, indicating the lower limit of Butler's approximate criterion for the required number of near-field microphones. It is a good criterion at values of L/λ smaller than 1.5, which is the range of source dimensions used by Butler in reference 8, but at shorter λ it considerably overestimates N.

Source Length

In the previous section we looked at the effects of changing acoustic wavelength on the required number of microphones for a fixed source length. To complete the analysis we should look into the effects of changing the length of a given number of multipoles, keeping the acoustic wavelength and radius of near-field microphones fixed. The results are summarized in figure 6, where N required for 1 dB accuracy is plotted against the length of the source distribution, L. The source distribution is composed of 31 random multipoles arranged in a fixed order. This figure shows that as L is expanded, more information (i.e., microphones) is needed to give an accurate extrapolation from the near field to the far field. Superimposed on figure 6 is the curve $N = 6L/\lambda$. It agrees with our data only at $L/\lambda = 1.5$, which is close to the dimensions of the source that Butler used to deduce his requirement of $6L/\lambda$.

On the basis of figures 5 and 6, we used curve fitting procedures that give us the following relationship for the required N for 1 dB accuracy

$$N_{min} = 6 \cdot L^{0.7}/\lambda^{0.8} \quad (9)$$

This relationship holds down to conditions where $N_{min} = 10$. For longer λ or smaller source lengths, or both, the lowest number should never be less than 10. There are two restrictions that should be emphasized. First, this relationship is for applications where both amplitude and phase information are available. For partially coherent noise sources the requirement is probably less than N_{min}. Second, this relationship is based on the configurations using discrete multipoles. If noise sources with radically different pressure distributions are used, then a similar analysis should be made to determine the dependence of N_{min} on L and λ.

Source-to-Microphone Distance

The source-to-microphone distance is another variable that was investigated. The linear distribution of 31 random multipoles of 3-m length was chosen as the noise source. The far-field points were taken on a semicircular arc of 50-m radius, with θ ranging from 5° to 175° at 5° increments. The microphones were also placed on a semicircular arc, but with θ (other than 5° and 175°) chosen not to coincide with those used in the calculation

of the exact far-field pressures. Microphone arc radii of 2, 5, 10, 20, 30, 40, 49, and 50 m were used. The results are shown in figure 7. In general, the increase in microphone radius has only a slight effect on predictive accuracy. Note that the only significant decrease in δSPL occurred for the case where $\lambda = 0.1$ m and $N = 40$. Here, any increase in N for the smallest radius of 2 m would have probably resulted in a substantial decrease in δSPL as indicated in figure 4. Even here, a 25-fold increase in the microphone distance reduces δSPL from 9.7 dB to only 4.7 dB. For all other cases there was a gradual, but not significant, decrease in δSPL.

We can interpret these results in terms of far-field and near-field pressure distributions such as those shown in figure 2. As the microphone radius increases, the shape of the pressure distribution measured by the array of microphones approaches that for the far field. Consequently, the insignificant changes indicate that the large disparity between shapes in the near field and far field is not of primary importance. Rather, it is probably the complexity in the pattern measured by the array of microphones and the resulting large number of significant terms in the expansion of equation (5) that require the large N.

Complexity of Pressure Distribution

It has been suggested that the complexity of the near-field patterns at shorter λ (fig. 2(b) and 2(c)) with their numerous valleys and peaks, may be responsible for the requirement of large N. To test this hypothesis, we used two different distributions of multipoles which would give us contrasting pressure patterns. The assumption of a linear distribution of 31 monopoles with randomly selected amplitudes gives us a pattern with many peaks and valleys (fig. 8); the assumption of a linear distribution of 31 lateral quadrupoles with randomly selected amplitudes gives us a pattern with fewer peaks and valleys (fig. 9).

The mean predictive errors for both configurations are shown in figure 10. Surprisingly, for small and moderate N, the mean predictive error is much larger for the less complicated distribution. An inspection of the values of δSPL for the distributed quadrupoles revealed several abnormally high values (25 to 50 dB) in the vicinity of $\theta = 90°$. Figure 9 shows that the exact far-field pressures in that region are very close to zero. Consequently, even small overestimates (compared with peak values) would result in large values for δSPL. In light of this situation, we modified the averaging process to give us a more realistic comparison. Based on the far-field patterns of figures 8 and 9, the local errors for θ between 80° and 110° were omitted from the averaging process for the quadrupole distribution; the local errors for θ between 100° and 110°, as well as 70° were omitted for the monopole distribution. The revised δSPL, compared in figure 11, show better predictive accuracy for the quadrupole distribution. However, the difference is not so large that we can unequivocally state that complexity in field patterns and the need for numerous near-field microphones go hand-in-hand.

What is needed is an analysis using a source configuration with a much smoother distribution than that shown in figure 9, one in which the sharp valleys are absent even at small values of λ; however, it may not be possible to find a finite distribution of point sources that will yield this type of pressure distribution. A continuous distribution of sources must be used. Consequently, one of our future goals is to conduct a similar analysis with a continuous distribution of sources modeled so that the resulting far-field pressure distribution will approximate that of a typical jet exhaust.

Microphone and Location Uncertainties

The second phase of our study is concerned with the effects of scatter in microphone data and imprecision in the location of the near-field microphones. We used the following approach to determine the effects of these errors. Again, we assume a linear distribution of multipoles so that we may calculate the exact near-field and far-field pressure amplitudes and phases. Then we assume a random distribution of errors in the near-field amplitudes, as well as errors in the coordinates of the near-field microphones. These errors are substituted into the near-field data. The modified near-field data are then used in the boundary-collocation computation of the far-field pressures. Finally, these approximated far-field pressures are compared with the previously calculated exact far-field pressures to determine the accuracy of the method. The predictive accuracy is again expressed in terms of the mean predictive error.

The scatter in microphone data was randomly chosen, with a maximum value of ±1 dB (approximately a 12% change in the pressure amplitude). This figure of 1 dB is based on our experiences with noise measurements in the Ames 40- by 80-Ft Wind Tunnel (1,2). Larry Russell (14) estimated that the microphones could be located within 1/4 in. in the Ames 40- by 80-Ft Wind Tunnel using conventional (i.e., non-coherent) optical equipment. Accordingly, we assume random errors in the radii and polar angles of the near-field microphone locations with a maximum of ±1 cm for the radius and ±1/3° for θ.

The results of this portion of the study are summarized in figures 12 through 14. At longer λ, the effects of microphone and location errors are relatively constant as N is increased. The microphone and location errors result in a 1-1/2 dB rise in δSPL at $\lambda = 1$ m, and a 2-1/2 dB rise in δSPL at $\lambda = 0.5$ m, indicating that the collocation coefficients become more sensitive to these errors as the wavelength is decreased. The oscillatory nature of the curve with both errors included (fig. 13), is caused by the random fashion in which these errors were introduced as the number of microphones was changed (values of δSPL were calculated for values of N in increments of 2 from 20 to 42).

The results shown in figure 14 for a wavelength of 0.2 were unexpected. The mean predictive error, due to microphone and location errors, no longer remained constant as N increased. At

N = 40, the combination of errors increased δSPL by 2 dB. But at N = 58, the combination of errors raised δSPL by 11 dB. Apparently, the crucial factor is the large order of the system of linear equations that leaves them vulnerable to an accumulation of errors. The small errors accumulate in a multiplicative sense, rather than an additive sense, completely destroying the predictive accuracy.

The question is, which error is responsible for the increase in δSPL, the microphone error or the location error? We calculated the effects of microphone error alone and the effects of location error alone for a few selected conditions. These results are also shown in figures 12 through 14. Before we discuss the results, we should point out that random errors are not additive. For example, if the randomly distributed errors due to the effects of one variable acting alone are much larger than those due to a second variable acting alone, then the random errors due to both variables acting together are only slightly larger than the errors due to the first variable acting alone.

For the longer wavelength, λ = 1 m. (fig. 12) the mean predictive error due to microphone error is larger than δSPL due to location error. Consequently, at longer wavelengths, it is the microphone error that is the source of the increased δSPL. At λ = 0.5 m, the microphone error and location error have roughly the same effect. For the shortest wavelength, λ = 0.2 m (fig. 14), the effect of location error is much larger than that for microphone error.

The situation at the shorter wavelengths can be improved in several different ways. One of these is to simply increase the near-field radius so that the relative location error is reduced. In figure 15, we compare the effects of location errors for a near-field radius of 2 m with that for a radius of 10 m. In the second case the maximum radial error is still ±1 cm, but the maximum angular error was reduced to ±1/18°. Figure 15 shows that this change has considerably reduced the mean predictive error for 58 microphones. Another method for reducing location errors is to use a dual laser system (14), whereby the location errors can be reduced to a few millimeters as compared to centimeters with non-coherent optical systems. The scatter in microphone data can also be reduced to ±1/2 dB by using longer time averaging.

Application

We will apply the results of our analysis to estimate the number of near-field microphones that should have been used for the Bies and Scharton experiment (10). In addition, we will estimate the effects of microphone and position errors. Bies and Scharton did not state the criterion that they used in choosing the number of microphones. However, their figure of 15 microphones is slightly greater than Butler's criterion of $N = 6L/\lambda$ (8). It should be pointed out that this criterion is only valid where simultaneous measurement of pressure amplitude and phase are made. For the case where only amplitude measurements are made, a larger number of microphones must be used.

In order to estimate the number of microphones required for near-field measurements of amplitude alone, let us make the following assumptions. First, the functional dependence of N on source length and wavelength, as given in equation (9), is unchanged. Second, we will account for the reduction in the number of measured variables by changing the constant of proportionality. In other words

$$N_{min} = K \cdot L^{0.7}/\lambda^{0.8} \qquad (10)$$

We can determine K from Butler's results in reference 9 for coherent sources. Predicted and exact far-field pressures were compared for two configurations. The first consisted of three monopoles of equal amplitude, emitting coherently, and separated by 0.25λ. We calculated the δSPL to be 5.6 dB. In the second configuration, the spacing between monopoles decreased to 0.125λ. For this configuration, we calculated an acceptable level for δSPL of 0.26 dB using nine microphones. Since this second combination of N and L/λ gives an acceptable value of δSPL, we will use the variables from this configuration to determine K.

The resulting constant, K, is 24. What this, admittedly empirical, approach says is that if the number of measured variables is reduced by a factor of two, then the number of microphones must be increased by a factor of four to maintain a given level of predictive accuracy. Using this constant, and applying equation (10) to the variables of reference 10 we find that $N_{min} = 26$ microphones. Figure 13 shows that microphone and location errors have not destroyed the predictive accuracy since the value for L/λ of 1.5 is still low. In our analysis in the previous section, we assumed a location error of 1 cm in a 2-m radius, or an error of 0.5%. Assuming the same level of locational accuracy for the experiment of reference 10, we should be able to predict the far-field pressures to within ±1 dB.

CONCLUSIONS

From the analysis presented here, the following conclusions can be made if we assume no uncertainties in microphone data or in the microphone location:

1. The only limitation on an accurate prediction of far-field pressures is the accuracy of presently available subroutines for solving systems of linear equations of large order, and for the computation of spherical Bessel functions.

2. Source-to-microphone distance has little, if any, effect on predictive accuracy.

3. Smaller numbers of microphones are required if the field patterns become less complex; however, the full extent of this improvement cannot be determined by the type of analysis described in this paper, where discrete point sources were used.

For the complex sources used in this study we have the following additional conclusions:

4. Where simultaneous measurements of near-field pressure amplitudes and phases are made, the minimum number of microphones required for accurate prediction is given by the empirical expression

$$N_{min} = 6L^{0.7}/\lambda^{0.8}$$

with a minimum of at least 10 microphones for very large λ or very small L.

5. For an acceptable number of microphones, say 50, accurate predictions are limited to values of L/λ no greater than 15.

If we assume imprecision in microphone data and in the location of those microphones, then we have the following conclusions:

1. Imprecision in the location of near-field microphones has a very large effect on predictive error. If we use standard wind tunnel instrumentation, then acceptable (±2-1/2 dB) predictions of far-field pressures can only be obtained for L/λ up to 10.

2. This restriction can be lifted to a large degree if we use more precise measurement techniques, such as dual laser arrangements, to locate the microphones.

3. The previous conclusions were based on the use of coherent sources. Partially coherent sources, which are typical of aircraft noise, are indicated in a previous study to be less restrictive in that fewer microphones are required to attain a given level of predictive accuracy. Consequently, the results of this paper indicate a lower limit to the predictive accuracy.

Acknowledgements: The authors express their sincere thanks to Mrs. Geraldine McCulley for the initial computer work, and to Mr. David Galant for his advice on the application of singular value decomposition.

APPENDIX

DISTINCTION BETWEEN REGIONS OF NEAR FIELD AND FAR FIELD

There is no precise boundary between the near field and the far field. There is only a precise definition of the far field. As the distance, R, from the source to the field point is increased, the far field is characterized as that region where: (1) the pressure amplitude decays as 1/R, and (2) the shape of the pressure distribution (i.e., the variation of p with θ for a fixed R), does not change as R is increased from one value to another.

However, pressure distributions at varying radii are not always readily available. As a consequence, we are sometimes forced to use imprecise criteria. The one commonly used is that R is in the far field if: (1) the ratio of R to the acoustic wavelength is larger than some number, n_λ, and (2) the ratio of R to the source length is larger than another number, n_L, where the n's are larger than unity. The question is, how large are the n's? There is no unique answer. The two numbers depend on the complexity of the sound source, as measured by its distribution, and the particular polar angle in that distribution. The numbers also depend on how precisely we want to approach the exact far field ($R = \infty$), since actual pressures approach the 1/R variation asymptotically.

We can get some idea of the magnitudes of n_L and n_λ by inspecting the data for the configurations of this study. We will first determine n_L from figure 16. This figure shows the sound pressure level plotted against the ratio R/L for three different polar angles. The configuration was chosen such that R/λ is 15 times larger than R/L, so that the far-field criterion is not determined by wavelength considerations. For each polar angle, a 1/R variation is superimposed upon the exact pressures using the 50-m point ($R/L = 16.67$) as a reference.

We will attempt to find some correlation between the shape of the near-field pressure distribution and the magnitude of the difference between the calculated pressure and the 1/R variation of pressure. For the top set of curves in figure 16, where $\theta = 34.8°$, the difference is relatively small with a ΔSPL of 3-1/2 dB at $R/L = 1$. For all practical purposes, the difference has disappeared at $R/L = 10$ (i.e., $n_L = 10$). For this case, figure 2(b) shows that the near-field pressure lies near a peak in the distribution. As θ is increased to 70.6°, the near-field pressure approaches a valley. Values of ΔSPL for the center set of curves become larger, although the difference still disappears at $R/L = 10$. At $\theta = 81.2°$, the bottom of a near-field valley is reached (fig. 2(b)). The resultant ΔSPL is extremely large with a value of 21-1/2 dB at $R/L = 1$. The calculated pressures do not reach far-field conditions until $R/L = 250$. From a strict interpretation, a value of $R/L = 250$ would be required for this configuration to completely attain far-field conditions. From a practical viewpoint, we should use a value of $R/L = 10$, which is more indicative of regions in the pressure distribution other than the valleys, as it is the pressures in these regions which are of importance in the subjective assessment of propulsion noise.

We will now look at a configuration in which wavelength considerations are more important than source length. The configuration was chosen such that R/L is 33 times larger than R/λ. Since the wavelength is much greater than the source length, the near-field and far-field distributions for this case are much smoother than those used in the previous case. The distributions are shown in figure 17. Note that there is only one valley of moderate depth for both distributions. The comparison of the calculated pressures and the 1/R variations in pressure are shown in figure 18, for three different polar angles. The 1/R variations used the 50-m point ($R/\lambda = 5$) as a reference. For the top two sets of curves ($\theta = 23.9°$ and $\theta = 156.1°$), the values of ΔSPL are very small. For all practical purposes, the difference in both cases has disappeared at $R/\lambda = 3$ (i.e., $n_\lambda = 3$).

Figure 17 shows that the pressures are not too far from peak values for both polar angles. The bottom set of curves in figure 18 shows larger values of ΔSPL. These larger values of ΔSPL are the result of the near-field pressure lying in the bottom of the valley as shown in figure 17. However, the magnitudes of ΔSPL (1-1/2 dB at $R/\lambda = 1$) are not too large as the valley is shallow. The difference in the calculated pressures and the 1/R variations has disappeared again at $L/\lambda = 3$. Because of the much smoother shape of the near-field distribution, we find that n_λ is smaller than n_L.

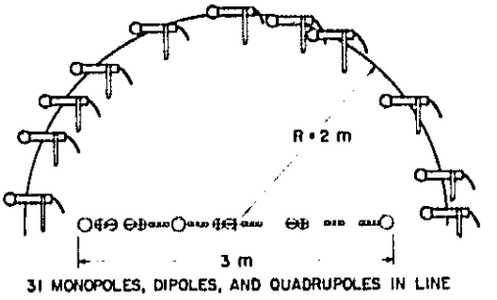

Figure 1.- Basic source-microphone configuration.

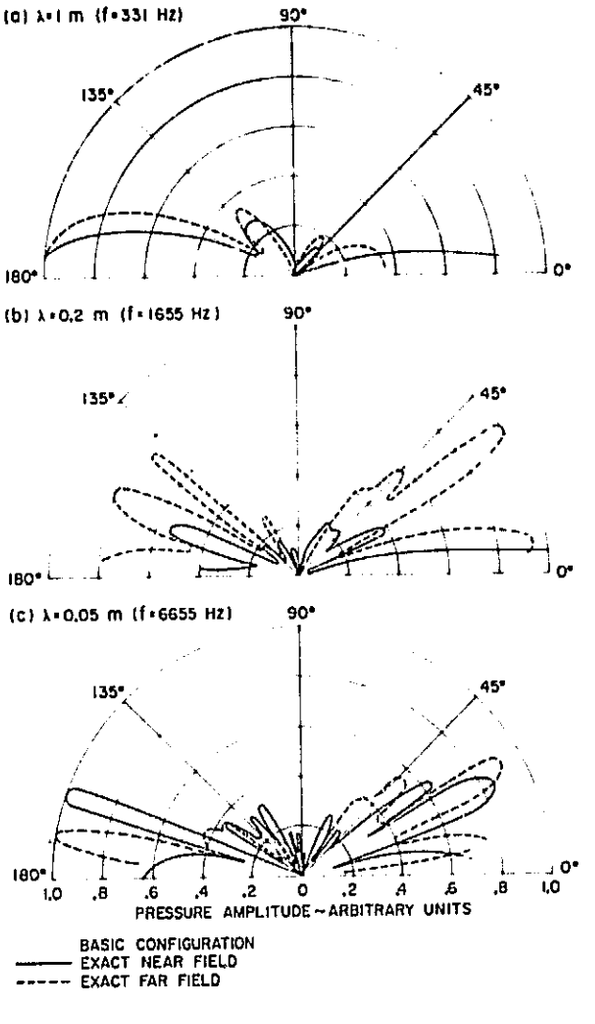

Figure 2.- Comparison of exact near- and far-field pressures.

REFERENCES

(1) A. Atencio, Jr. and P. T. Soderman, "Comparison of Aircraft Noise Measured in Flight Tests and in the NASA Ames 40- by 80-Foot Wind Tunnel", AIAA PAPER NO. 73-1047, Oct. 1973.

(2) A. Atencio, Jr., "Wind Tunnel Measurements of Forward Speed Effects on Jet Noise From Suppressor Nozzles and Comparison With Flight Test Data", AIAA PAPER NO. 75-870, June 1975.

(3) F. A. Wilcox, "Comparison of Ground and Flight Test Results Using a Modified F106B Aircraft", NASA TM X-71439, Nov. 1973.

(4) D. A. Bies, "Investigation of the Feasibility of Making Model Acoustic Measurements in the NASA Ames 40- by 80-Foot Wind Tunnel", NASA CR-114352, July 1971.

(5) P. T. Soderman, "Instrumentation and Techniques for Acoustic Research in Wind Tunnels", to be presented at 6th International Conference on Instrumentation in Aerospace Simulation Facilities, Ottawa, Canada, Sept. 1975.

(6) W. J. Moggs, A Practical Method of Predicting Far-Field Acoustic Pressure From Measurements Near the Source", U.S.N. Marine Eng. Lab. Tech. Memo 442/65, Nov. 1965.

(7) J. L. Butler, "A Series Expansion Method for the Prediction of the Far-Field From Near-Field Measurements", Parke Math. Lab. Tech. Memo. No. 1, Dec. 1967.

(8) J. L. Butler, "Solution of Acoustical-Radiation Problems by Boundary Collocation", J. ACOUST. SOC. AMER. VOL. 48, pp. 325-336, 1970.

(9) J. L. Butler, "A Method for the Prediction of the Far-Field From Near-Field Measurements of the Amplitude Alone", Parke Math. Lab. Tech. Memo. No. 3, May 1969.

(10) D. A. Bies and T. D. Scharton, "Relation Between Near-Field and Far-Field Acoustic Measurements", NASA CR-114756, Mar. 1974.

(11) D. C. Galant, Private Communication, Jan. 1974.

(12) G. H. Golub and C. Remisch, "Singular Value Decomposition and Least Squares Solutions", NUMBER MATH., VOL. 14, pp. 403-420, 1970.

(13) J. M. Varah, "On the Numerical Solution of Ill-Conditioned Linear Systems With Applications to Ill-Posed Problems", SIAM J. NUMBER ANAL., VOL. 10, pp. 257-266, April 1973.

(14) Larry Russell, Private Communication, June 1974.

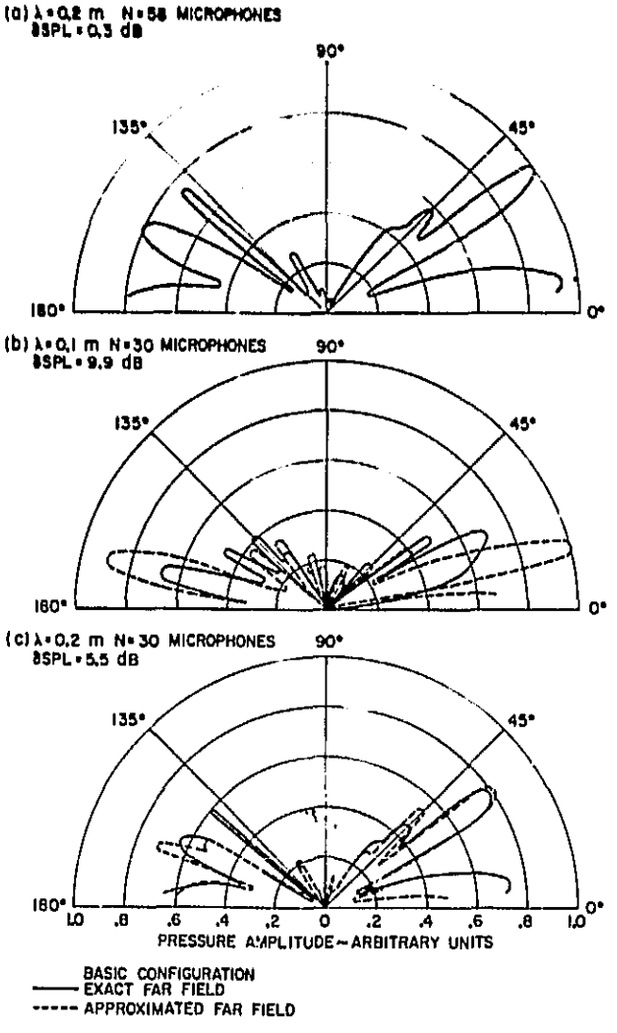

Figure 3.- Comparison of exact and predicted far-field pressures.

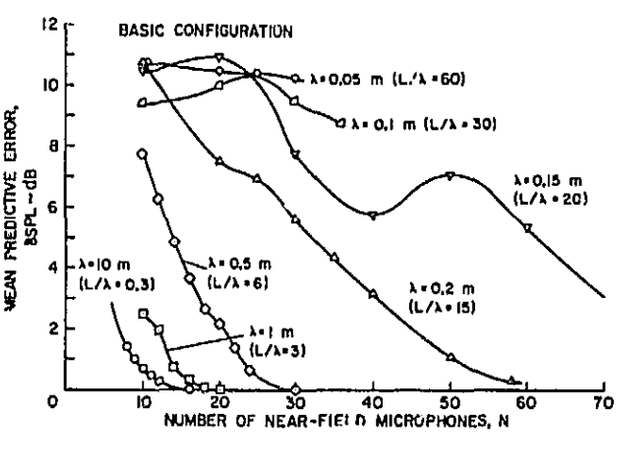

Figure 4.- Effect of number of near-field microphones on far-field predictive accuracy.

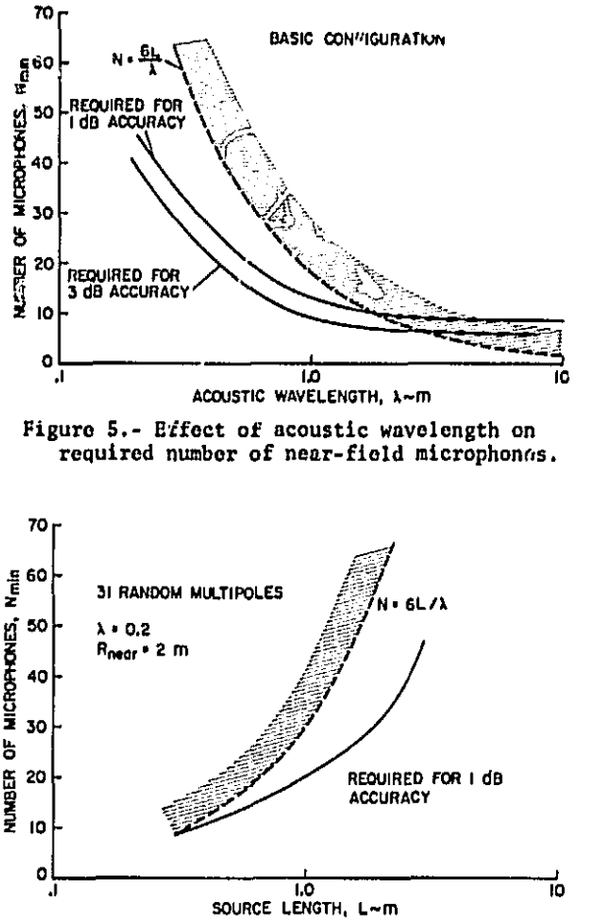

Figure 5.- Effect of acoustic wavelength on required number of near-field microphones.

Figure 6.- Effect of source length on required number of near-field microphones.

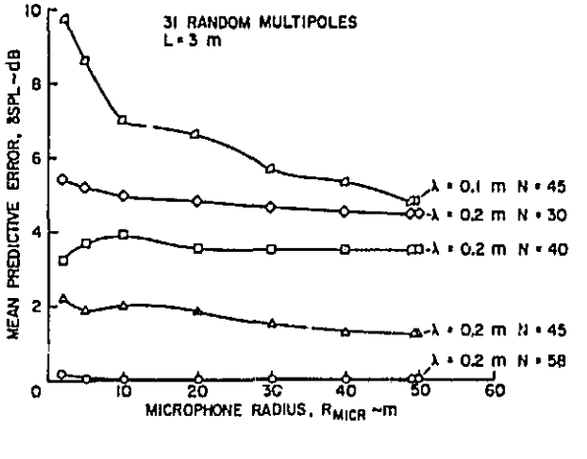

Figure 7.- Effect of microphone radius on far-field predictive accuracy.

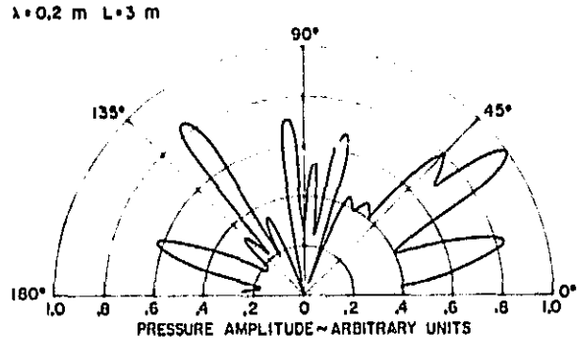

Figure 8.- Exact far-field pressures for distribution of 31 random monopoles.

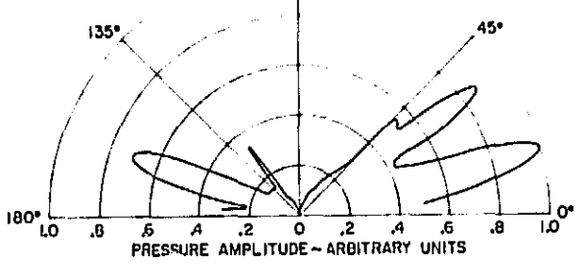

Figure 9.- Exact far-field pressures for distribution of 31 random quadrupoles.

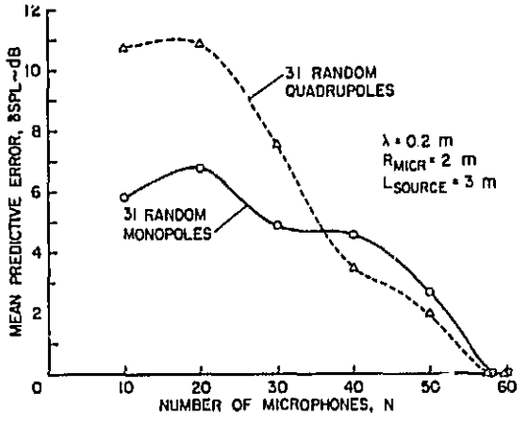

Figure 10.- Comparison of predictive accuracy for monopole and quadrupole distributions.

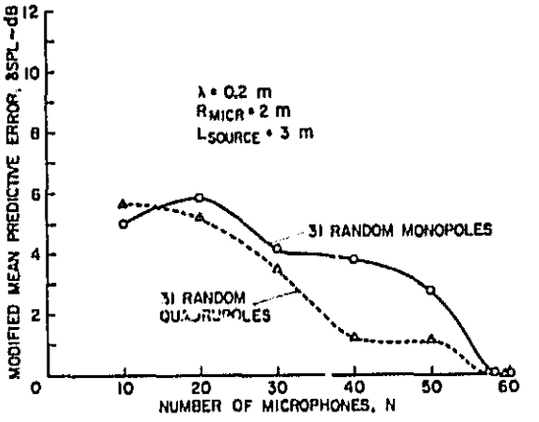

Figure 11.- Comparison of predictive accuracy for monopole and quadrupole distributions using a modified mean predictive error.

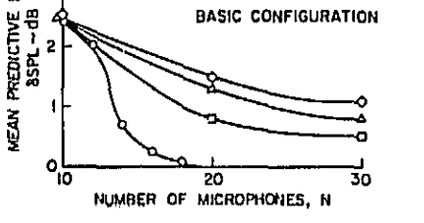

Figure 12.- Effect of microphone and location errors on predictive accuracy at $\lambda = 1$ m.

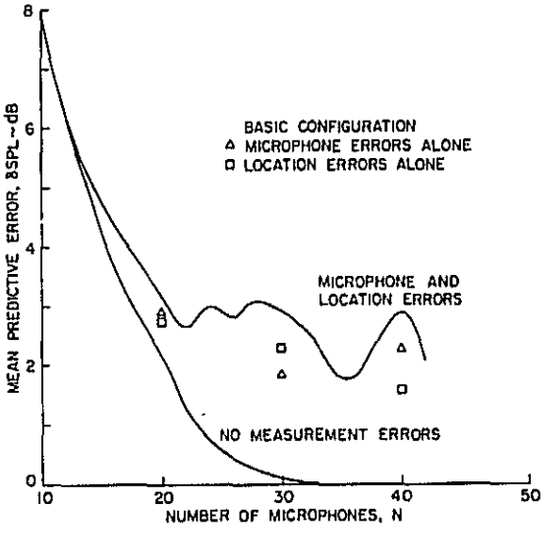

Figure 13.- Effect of microphone and location errors on predictive accuracy at $\lambda = 0.5$ m.

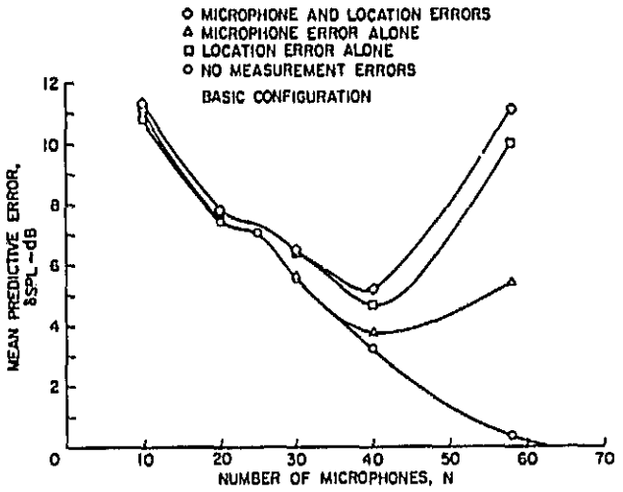

Figure 14.- Effect of microphone and location errors on predictive accuracy at $\lambda = 0.2$ m.

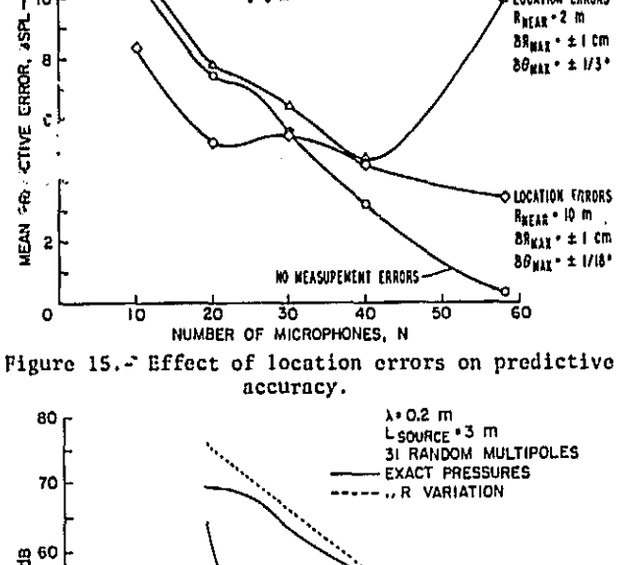

Figure 15.- Effect of location errors on predictive accuracy.

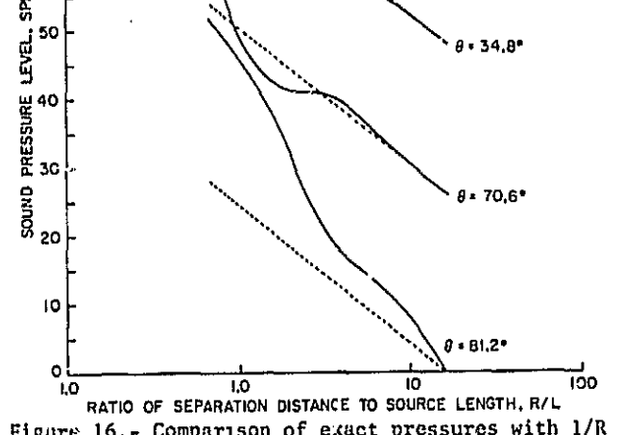

Figure 16.- Comparison of exact pressures with 1/R variation for source length dependency.

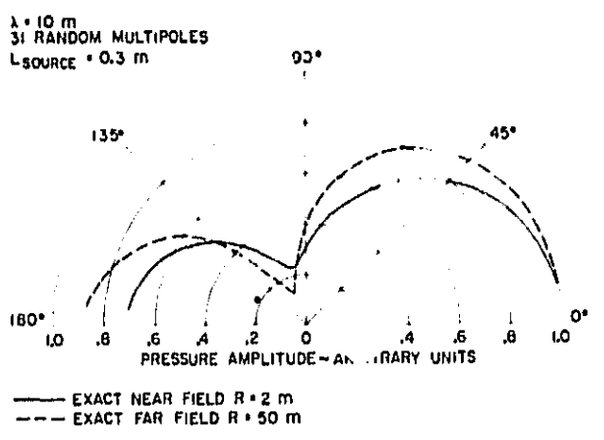

Figure 17.- Comparison of exact near field and far-field pressures.

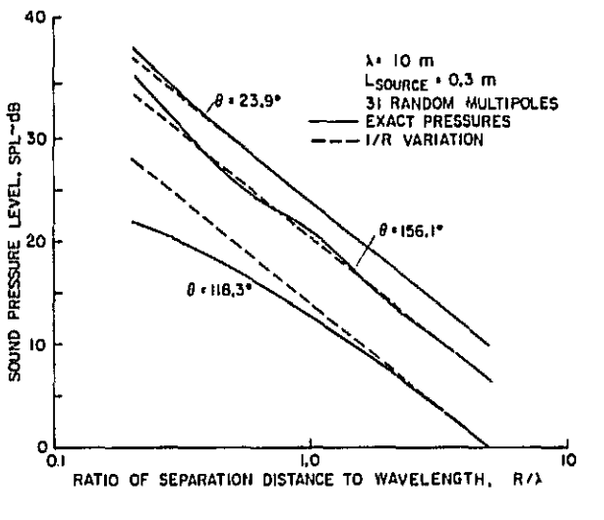

Figure 18.- Comparison of exact pressures with 1/R variation for wavelength dependency.